NUMERICAL SIMULATION OF TURBULENT FLOWS
IN COMPLEX ENGINE GEOMETRIES

J.Y. Tu[*]

The Royal Institute of Technology

S-100 44, Stockholm, Sweden

Abstract

Flows in complex engine geometries are simulated by a developed computational methodology combining overlapping grids with multigrid methods. The flow is modeled by the three-dimensional incompressible Navier–Stokes equations incorporating a k-ε turbulence model. The governing equations are discretized in the physical space using a finite volume method on a semi-staggered grid. The multigrid method is used to accelerate the convergence of the numerical solver. The main feature of the present method is its extended flexibility to deal with three-dimensional complex multicomponent and time-dependent geometries. The flexibility and potential of the current method has been demonstrated by calculating several cases which would be very difficult to be handled by other approaches.

I. Introduction

Computational fluid dynamics (CFD) is becoming an essential tool in the understanding of fluid physics and in engineering design. Practical and engineering problems in CFD inevitably involve complex geometries. In order to obtain realistic and usable results, the flow fields to be computed are often complex and the calculations must often be made in a complicated, time-dependent, three-dimensional (3-D) geometry. A typical example for such a geometry that has been discussed in this paper is an internal combustion (IC) engine. Figure 1 shows a conventional diagram of an IC engine configuration.

The flow motion within the cylinder is one of the most important factor controlling the combustion process. It has also been shown experimentally that the flow structure inside the engine cylinder dependents strongly on the geometry of the intake/exhaust port system, including the seat angle and the lift of moving valves, the location of the intake/exhaust axis with respect to the cylinder centreline and the geometry of the piston face, including the different sort of the bowel-in-piston.[1] Therefore, a good understanding of fluid motion inside the engine cylinder is critical in developing new engine designs with the improved operating and emissions characteristics.

The objective of this work is to develop a new computational methodology which inculdes a numerical technique that can readily treat more realistic engine configurations and a numerical procedure that is robust and efficient for complex engine flow calculations. The main feature of this computational methodology is the use of an overlapping grid technique, a time-independent grid system, the finite volume approach and multigrid methods. The overlapping grid allows the easy treatment of complex geometries including the motion parts in the domain and makes it possible to handel realistic engine configurations. The multigrid method is incorporated into the overlapping grid technique to allow the efficient solution of discrete problems. The finite volume method and semi-staggered grid system are used to approximate the governing equations on complex domains. The current code using all the numerical methods mentioned above offers great flexibility and efficiency in treating complex engine problems.
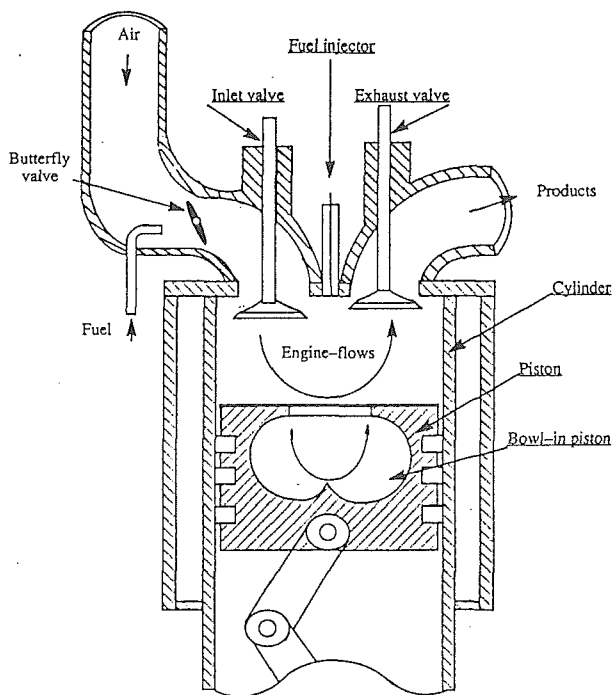

Fig.1 Illustration of an internal combustion engine

---

* Graduate student, Department of Gasdynamics

At this stage, the incompressible nonreacting flows are assumed. The flow is modeled by 3–D time–dependent incompressible Navier–Stokes equations incorporating a k–ε turbulence model. The performance of the present method has been validated by comparing results with those from exact solutions and those from experiments. The flexibility and potential of the present code has been demonstrated by calculating several cases which would be very difficult to be handled by others.

II. Formulation of the physical problem

A. Governing equations

For three–dimensional incompressible turbulent flows, the dimensionless Reynolds averaged Navier–Stokes equations and the continuity equation, in Cartesian coordinates can be written in dimensionless, conservative form as follows:

$$\frac{\partial U}{\partial t} + \nabla \cdot UU = -\nabla P + \nabla \cdot (\frac{1}{R_{eff}} \nabla U) \qquad (1)$$

$$\nabla \cdot U = 0 \qquad (2)$$

where $U=(u,v,w)$ is the mean velocity in x–, y– and z–directions, respectively; t indicates the time; P expresses the mean pressure.

For turbulence closure,[2] the model is composed of two equations, for the non–dimensional turbulence kinetic energy k and its rate of dissipation ε are as follows:

$$\frac{\partial k}{\partial t} + \nabla \cdot Uk = \nabla \cdot (\frac{1}{R_k} \nabla k) + G - \epsilon \qquad (3)$$

$$\frac{\partial \epsilon}{\partial t} + \nabla \cdot U\epsilon = \nabla \cdot (\frac{1}{R_\epsilon} \nabla \epsilon) + \frac{\epsilon}{k}(C_1 G - C_2 \epsilon) \qquad (4)$$

where G is the rate of generation of turbulence kinetic energy[17] The effective viscosity which the effective Reynolds numbers base on are difined by

$$\nu_{eff} = \nu_l + \nu_l \ ; \quad \nu_k = \frac{\nu_l}{\sigma_k} + \nu_l \ ; \quad \nu_\epsilon = \frac{\nu_l}{\sigma_\epsilon} + \nu_l \qquad (5)$$

ν_l is laminar viscosity. The eddy viscosity ν_l is classically given by

$$\nu_l = C_\mu \frac{k^2}{\epsilon} \qquad (6)$$

This model contains five empirical constants which assume the following values:[3]

$C_\mu = 0.09; \ C_1 = 1.44; \ C_2 = 1.92; \ \sigma_k = 1.00; \ \sigma_\epsilon = 1.30$

B. Boundary conditions

There are potentially different types of boundaries, such as solid surfaces, inlets/outlets and 'internal surfaces'. No–slip condi-

tion is applied on solid surfaces. The velocity at the piston face is equal to the piston velocity and the inlet velocity can be obtained from the overall mass balance by[4]

$$V_{io} = S_{piston}(\pi D^2/4)/A_e \qquad (7)$$

where S_{piston} is the piston speed; D the cylinder diameter and A_e the effective intake area.

The turbulence kinetic energy, k, at the inlet is scaled by the mean velocity there, while the dissipation rate ε is tied to the port diameter.[5] The velocity components, k and ε at the 'internal' boundary points are computed by interpolation during the iterative process. A three–dimensional Lagrange interpolation scheme is used and is implemented as a sequence of three one–dimensional interpolations. It should be noted that this kind of interpolation scheme does not guarantee global mass conservation before convergence. For incompressible flows it has been found that adding a correction to the interpolated values could improve the convergence rate without affecting the finial solution.[6]

The following 'wall' functions are used for k and ε to bridge the near–wall region:[2]

$$k_p = C_\mu^{-1/2} U_\tau^2 \qquad (8)$$

$$\epsilon_p = U_\tau^3/(\kappa y_p) \qquad (9)$$

where U_τ is the wall shear velocity, computed by

$$U^+ = y^+ \qquad \text{for } y^+ \leq 11.63$$

$$U^+ = \ln(Ey^+)/\kappa \qquad \text{for } y^+ > 11.63$$

$$U^+ = U_p/U_\tau \ , \qquad y^+ = U_\tau \, y_p \, /\nu_l$$

here the subscript p refers to the grid node next to the wall; y_p is the distance normal to the wall; k and E are the constants from the law of the wall, with values of 0.4187 and 9.793, respectively.

C. Initial conditions

For the engine problem, the flow is time–dependent. At t=0, the piston is stationary at the top dead center (TDC) of the cylinder and the flow everywhere is set to be at rest. Initial turbulent kinetic energy and the dissipation rate are scaled to the mean piston speed.[5] The flow inside the cylinder is driven by the motion of the piston away from TDC, according to simple harmonic motion, i.e. the motion of the piston follows a cosine wave while its velocity follows a sine wave. The position of the moving piston is deierminated by

$$Z = L_c + \frac{L_s}{2}[1 - \cos(2b\pi t)] \qquad (10)$$

where L_c is the clearance height of the cylinder and it is taken as $L_s/L_c = 5$; $2b\pi t$ refers to the crank angle θ where b is the engine speed. Here the piston stroke is $L_s/D = 1.0$ and the cylinder bore is $D = 1.0$

III. Method of solution

A. Overlapping grids

A overlapping grid is constructed to cover the region on which governing equations are to be solved. The basic idea of the overlapping grid technique used here is to employ a separate body-fitted grid for each component in a multicomponent configuration and then to interface the grids in a manner which allows for efficient solution of governing equations. One of the main advantages of using overlapping grids is that it can reduce the topological complexity of a complicated geometry, permitting each component to be more easily fitted with an appropriate grid. Usually, such an appropriate grid is one type of the existing structured grid. The six basic mesh types (see Fig. 2) are now available in the present code, to be generated and combined for various of 3-D complex configurations. Comparing with the patched grids or multi-block technique, the overlapping grids are more flexible for the multicomponent configuration since completely differently orientated grid systems, such as O-O and H-O type mesh, can be mixed.
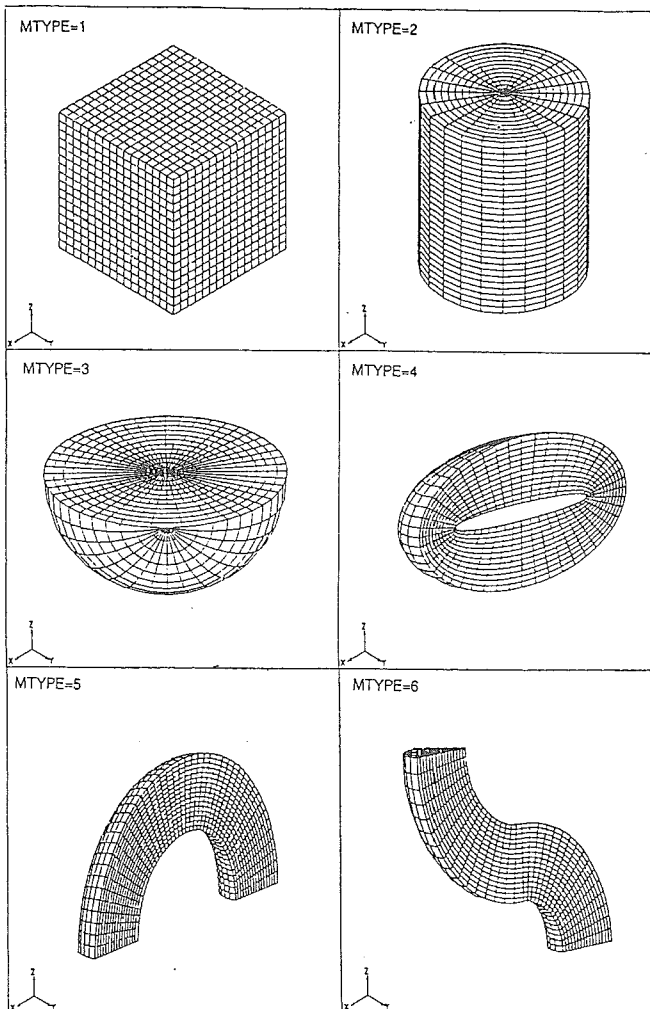

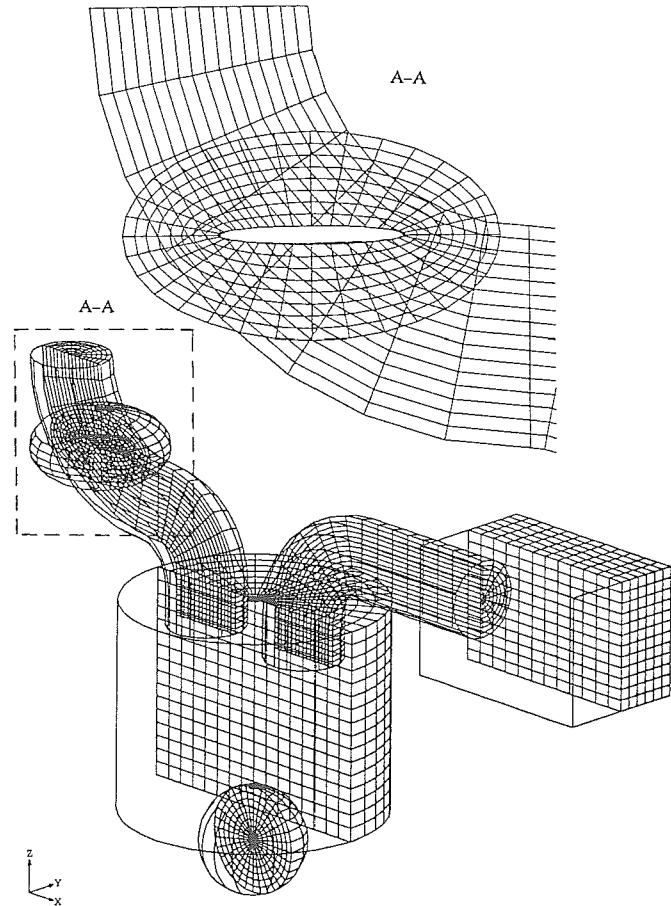Fig.2 Illustration of six basic structured mesh types

Fig.3 A 3-D view of overlapping grid system for a more realistic engine configuration

An example which uses all of these six basic structured grids for an engine configure is displayed in Fig.3. In this example, six local body-fitted grids are generated for a cylindrical combustion chamber, an S-type intake port, a curved-duct exhaust port, a spherical bowl-in-piston, a butterfly valve and a rectangle container at the exhaust. They are combined together and overlapping where they meet. The grid points on one mesh which lie inside the butterfly valve are flagged as unused points which are excluded from the computation. The internal boundary points are defined on the overlapping region between the two grids for interfaces by interpolation. The data for these internal boundary points in different grids are organized to be stored in additional one-dimensional arrays and are independently managed by an auxiliary pointer system.

The interpolation is implemented in the transformed space (r, s, t). A Newton method[7] is used to locate the interpolated point on the transformed space. The Newton method used here is to set up an iteration matrix derived from the Taylor series expansion around the point of interpolation. The distance between the interpolated point and its nearest neighbouring grid point on the transformed space are computed by the iteration. The Lagrange interpolation formulation is then used in the three spatial directions

$$\phi_{intp} = \sum_{r=1}^{n+1} \sum_{s=1}^{n+1} \sum_{t=1}^{n+1} \left(\prod_{\substack{k=1 \\ k \neq r}}^{n+1} \frac{x - x_k}{x_r - x_k} \right) \left(\prod_{\substack{m=1 \\ m \neq s}}^{n+1} \frac{y - y_m}{y_s - y_m} \right) \left(\prod_{\substack{p=1 \\ p \neq t}}^{n+1} \frac{z - z_p}{z_t - z_p} \right) \phi_{rst} \qquad (11)$$

where ϕ_{intp} is the function value of interpolated point and ϕ_{rst} are the function values of selected points for interpolation; n is the interpolating order which is taken to be 1, 3, 5, ..., etc.

Compared with the single grid approach, the storage of numerical data for the overlapping grid system is more complicated. The data structure that we employ here is an extension of the multigrid data structure[8]. All the dependent variables and the grid parameters are stored in one-dimensional arrays. A pointer system is defined so that each sub-grid can be accessed directly by a pointer. The position of the first variable entry of each sub-grid is stored and can be easily retrived. The data is organized by grid levels as in the case of the multigrid scheme. The data for internal boundary points in different sub-grids are also stored in additional shorter one-dimensional arrays and are independently managed by an auxiliary pointer system. Our numerical experience shows that this type of data structure allows access to each sub-grid independently and it is easy to deal with the interfaces among the different grids. This grid system allows also addition/deletion of locally refined sub-grids.[9]

It should be noted that a moving boundary (e.g. a moving piston in an IC engine) has been specially treated in the present overlapping grid system. The moving piston is artificially treated as a variable solid body in the computational domain. An overlapping grid system is first generated for the piston lying at the bottom dead center (BDC) where the size of body disappears. When the piston moves towards TDC or from TDC to BDC, the size of the body will vary with the motion of piston. Figure 4 shows two different positions of the piston and their corresponding overlapping grid system. It can be seen that during the solution the grid system doesn't change with the motion of the piston. Only those grid points lying in the piston body will be flagged as unused points which are excluded from the calculation. When the piston face does not exactly lie on a grid plane, a local computational region, i.e. a thinner cell layer as illustrated in Fig.4, is allowed to attach to the piston. The main advantage of this grid system is that no mesh regeneration is required even when different parts move relatively to each other.
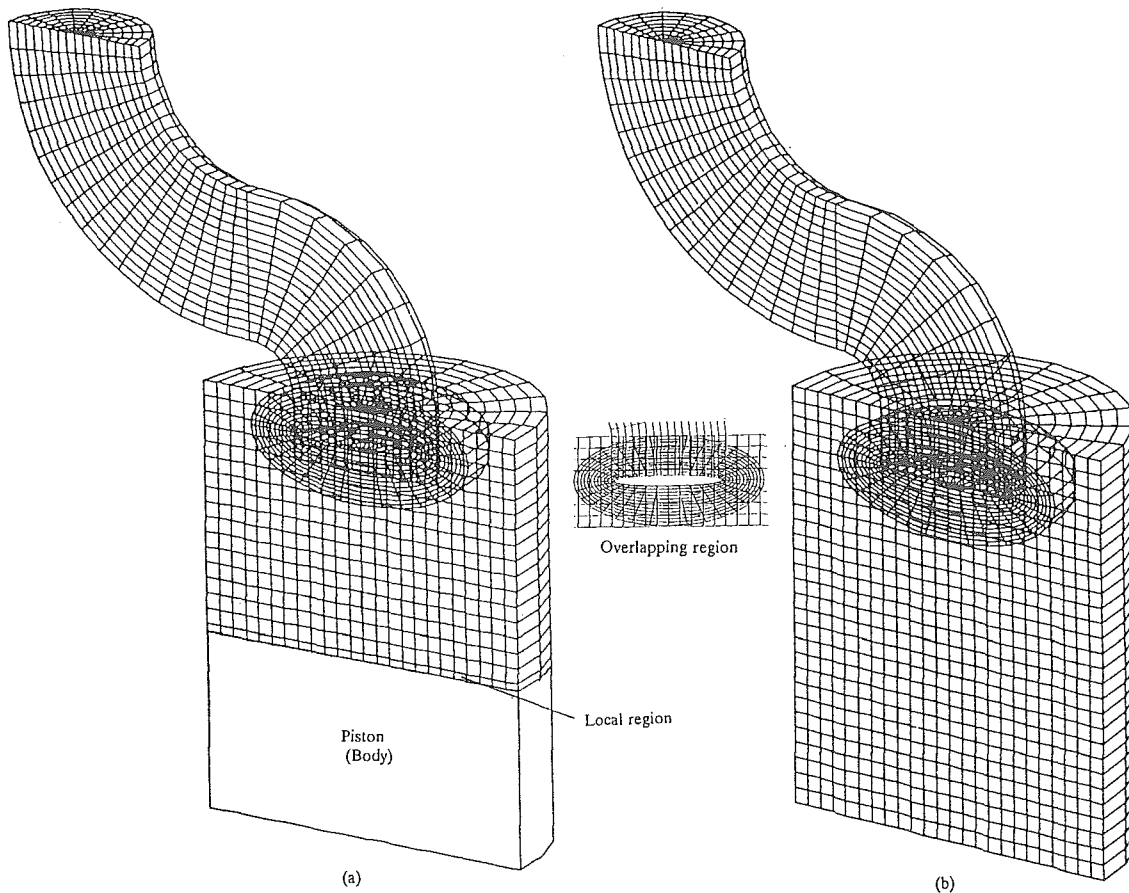

Overlapping region

Local region

Piston (Body)

(a)

(b)

Fig.4 A 3-D view of time-independent grid system for moving piston
(a) at a crank angle of θ = 90 deg (b) at a crank angle of θ = 180 deg

B. Numerical procedure

A second order accurate finite volume (FV) method is used to discretize the partial differential equations using cartesian velocity components. By this approach one avoids the need for transformation of coordinates and it makes the information exchange procedure among different grids simpler. We adopt a semi-staggered grid system in which all velocity components are defined at the cell vertex while other scalar quantities, such as, pressure, turbulent kinetic energy and dissipation rate are defined at the cell centre. The main advantage of using a semi-staggered grid system is that one does not have to specify boundary conditions on the pressure. The control volume for the continuity equation (2) and the turbulent scalar transport equations (3) and (4) is the cell element itself. For the momentum equations, the control volume is formed by joining the cell centres surrounding the point of calculation. Wedged-shaped control volumes are used in cases of degeneration (as near the axis of cylindrical coordinates). For details of the discretization by using FV approximations see e.g. reference 10.

It is well known that non-staggered and semi-staggered arrangements of variables (such as, using FV approximations) experience odd/even decoupling for both linear and nonlinear problems. These high frequency oscillations can be damped by a fourth order difference operator which is similar to the scheme proposed by Jameson[11].

The discrete formulation of the governing equations is implicit in time and the MG procedure is used to accelerate the convergence of the solution in each time step. The algorithm of the MG technique is to construct a hierarchy of grids with different mesh sizes. An appropriate relaxation scheme is used as a 'smoother' on each level to quickly reduce the amplitude of high-frequency error components which cannot be approximated on the next coarser grid. The 'smoothed' solution is then transferred to the next coarser grid to further eliminate error components with longer wavelengths. By employing several levels of grids, one is able to solve for the high-frequency components on a fine grid and for the low-frequency components on a coarse grid. As a result, the overall convergence rate is greatly accelerated. A volume averaging restriction operator is empolyed for the residuals and the dependent variables are according to FAS model.[12] The corrections on the coarse grids are interpolated trilinearly to fine grids. The iterations are carried out by a V-cycle MG process until a converged solution is obtained.

It should be noted that by using the basic Schwarz algorithm the discrete equations in each zone are solved before updating all the internal boundaries and the procedure is repeated until convergence is achieved. Previous numerical experiences[13,14] indicate that such an iterative process results in slow convergence and is sensitive to the extent of the overlap. Here, the use of the smoothed approximation for the interzonal exchange is an integral part of the MG cycle.

IV. Result and discussion

A. An engine-like geometry

In order to validate the current code for multicomponent geometries, a case is chosen where there are four componets, which are a cylindrical combustion chamber, an S-type intake port, a curved-duct exhaust port and a bowl-like sphere, respectively. The overlapping grid system for this case is similar to that shown in Fig.3. We solve two coupled partial differential equations (i.e. simulating a two equation model of turbulent flows) with a given shape of test functions, k and ϵ:

$$k = 1.5 + \cos(2\pi x)\cos(2\pi y)\cos(2\pi z)\cos(2\pi t)$$

$$\epsilon = 1.5 + \sin(2\pi x)\sin(2\pi y)\sin(2\pi z)\cos(2\pi t)$$

The velocity field, needed in the convective terms is assumed to be given. The system of equations is coupled through the forcing terms on the right hand-sides and the diffusion coefficient as in the k-ϵ model:

$$S_k = -\varrho\epsilon + S_k'$$

$$S_\epsilon = -C_1\frac{\epsilon^2}{k} + S_\epsilon'$$

$$\frac{1}{R_k} = \frac{1}{R_\epsilon} = C_2\frac{k^2}{\epsilon}$$

where C_1 and C_2 are constant, S'_k and S'_ϵ are the balancing terms of the two equations obtained by substituting the test functions for k and ϵ, respectively.

A steady solution for k field is shown in Fig. 5 (a). A steady liminar flow in this type of geometry is also simulated by solving Navier-Stokes equations and computed flow field in a symmetrical plane is displayed in Fig. 5 (b). In this calculation, the uniform flow profiles are set at all the inlets and outlets by balancing the global mass flux. The Reynolds number (based on the inlet characteristic parameters) is 50.

B. A case with an S-type intake port and a fixed valve

A second example is chosen to demonstrate the capability and potential of the present method for predicting flows in a complex domain where a global single grid is too difficult to cover it. The engine configuration consists of a cylindrical combustion chamber with a moving piston, an S-type intake port and a fixed valve. Each part is fitted by a local body-fitted mesh and its overlapping grid system has been illustrated in Fig. 4. The Reynolds number, based on the maximum piston velocity and the chamber diameter, is taken to be Re = 5200. The finest grids used are 13x26x29 for the chamber, 9x22x33 for the intake port and 13x26x21 for the valve, respectively. In the numerical calculation, it is assumed that the valve is fully opened during the entire intake process.

(a)

(b)
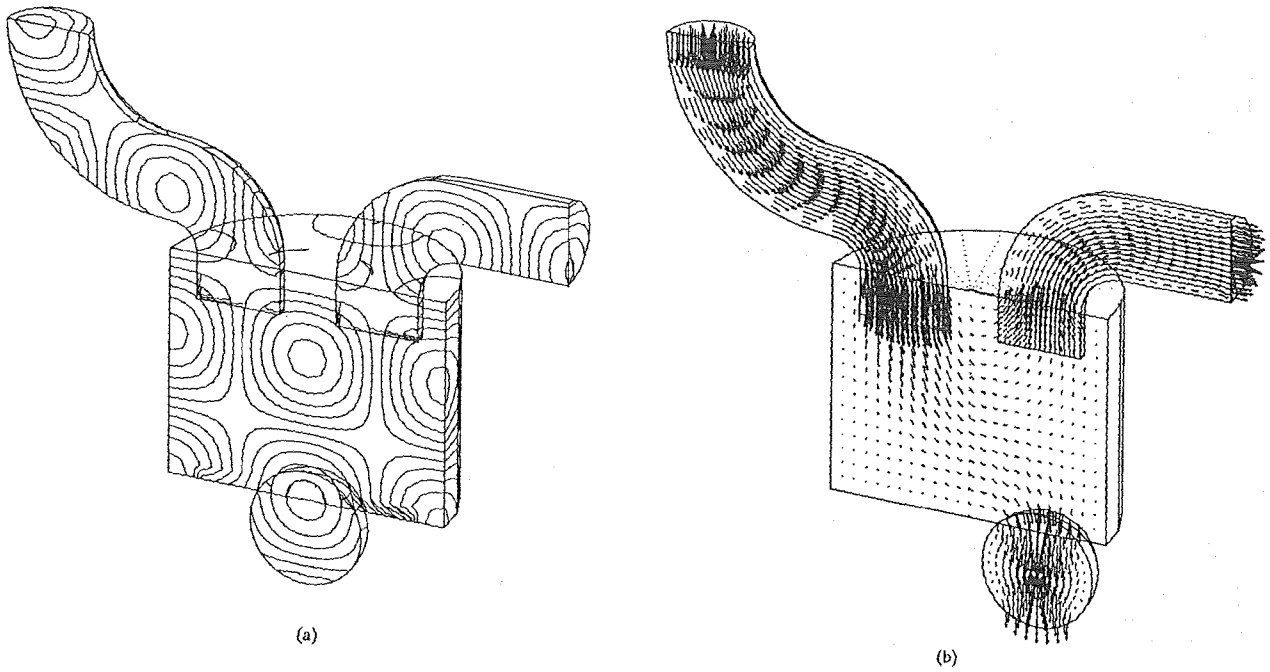
Fig. 5   Computational fields in a symmetrical plane
(a) Steady k field   (b) Steady liminar flow field
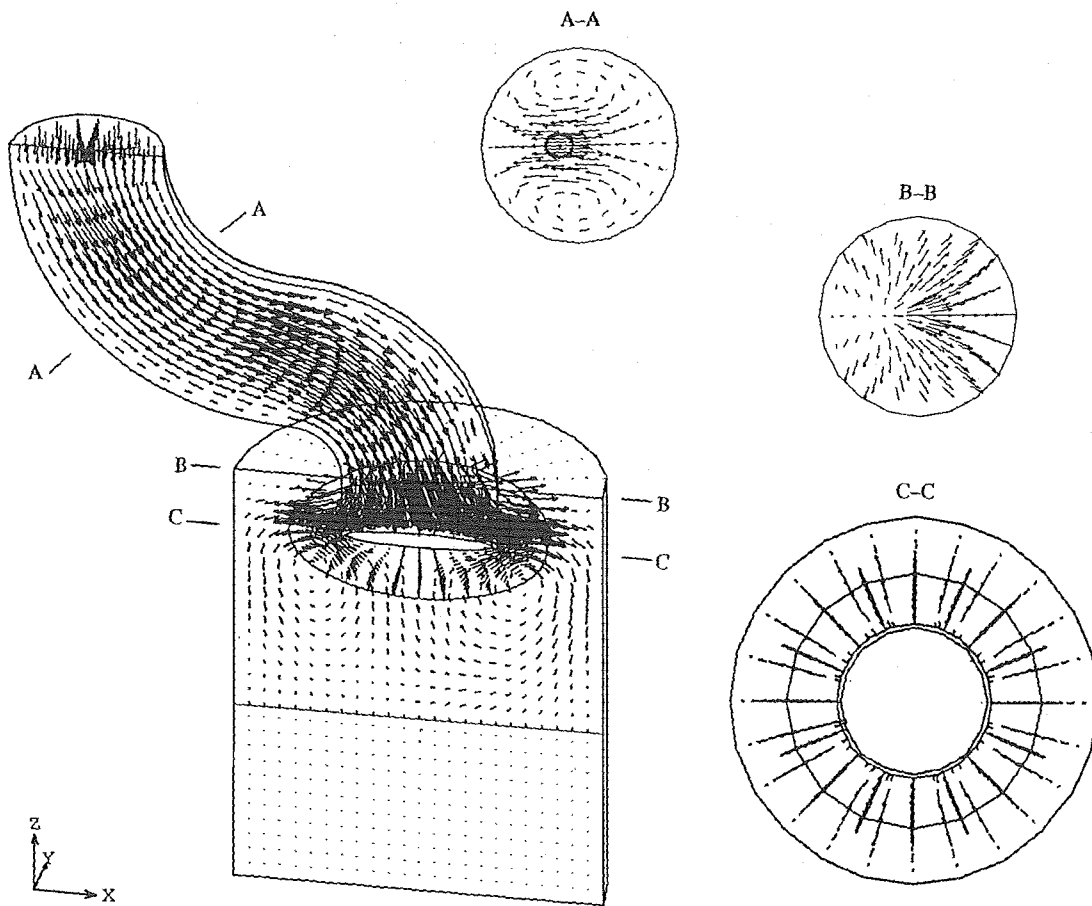

A–A

B–B

C–C

Fig. 6   A 3-D view of velocity field in a symmetrical plane

1748

Figure 6 shows a three-dimensional velocity vector plot of the intake stroke flow at an equivalent crank angle $\theta = 90$ deg. The interaction of the intake jet with the valve and then with the wall produces large scale rotating flow patterns within the cylinder volume. It is interesting to see that an unsymmetrical rotating flow is formed due to the directed intake port. This feature is strongly similar to that observed experimentally by Sanatian.[15] The recirculation flow with the twin counter-rotating vortices in the middle of the intake port and the inlet flow with a tangential momentum are also depicted in Fig. 6.

V. Concluding remarks

The flow field in complex engine geometries has been investigated numerically. The flow is governed by three-dimensional, time-dependent, incompressible Navier-Stokes equations incorporating a k-ε turbulence model. The use of a numerical scheme combining an overlapping grid technique with a multigrid method and the use of a time-independent grid system for the moving piston in IC engines are emphasized. The validity of the current code is sucessfully demonstrated by comparing the computed results with the available experimental data and exact numerical solution. Two cases which are geometrically close to the realistric engine configurations are chosen to demonstrate the capability and potential of the currently developed method.

Acknowledgment

References

[1]Gosman, A.D., "Computer Modeling of Flow and Heat Transfer in Engines, Progress and Prospects," *JSME, Int. Symp. on Diagnostics and Modeling of Combustion in Reciprocating Engines*, Tokyo, 1985, pp. 15-26.

[2]Launder, B.E. and Spalding, D.B., "The Numerical Computation of Turbulent Flow," *Comp. Meth. in Appl. Mech. and Eng.*, Vol. 3, 1974, pp. 269-289.

[3]Grasso, F. and Brocco, F.V., "Computed and Measured Turbulence in AxiSymmetric Reciprocating Engines," *AIAA Journal*, Vol. 21, 1983, pp. 601-607.

[4]Tu, J.Y. and Fuchs, L., "Application of Overlapping Grids to 3-D Flow Calculations in a Model Engine," *Numerical Methods in Laminar and Turbulent Flows*, (Eds., C. Taylor, et al.), Pineridge Press, 1991, pp. 1198-1208.

[5]Jennings, M.J. and Morel, T., "Observations on the Application of the k-e Model to Internal Combustion Engine Flows," *Combust. Sci. Technol,.* Vol. 58, 1988, pp. 177-193.

[6]Gu, C.-Y. and Fuchs, L., "A Non-Isotropic Interpolation Scheme Applied to Zonal-Grid Calculation of Transonic Flows," *Numerical Methods in Laminar and Turbulent Flows-VI*, (Eds., C. Taylor, et al.), Pineridge Press, 1987, pp. 975-989.

[7]Tu, J.Y., "Three-Dimensional Overlapping Grids and Multigrid Methods for Flow Calculations in Complex Engine Geometries," Thesis of Dr. Eng. (Preparing), Gasdynamics Department, Royal Institute of Technology, Sweden, (1992).

[8]Fuchs, L. and Zhao, H.S., "Solution of Three-Dimensional Viscous Incompressible Flows by a Multi-Grid Method," *Int. J. Numer. Methods Fluids*, Vol. 4, 1984, pp. 539-555.

[9]Fuchs, L., "A Local Mech Refinement Technique for Incompressible Flows," *Computers & Fluids*, Vol. 14, 1986, pp69-81.

[10]Tu, J.Y. and Fuchs, L., "Overlapping Grids and Multigrid Methods for Three-Dimensional Unsteady Flow Calculations," to be published in *Int. J. Numer. Methods Fluids*.

[11]Jameson, A., "Numerical Solution of the Euler Equation for Compressible Inviscid Fluids," *Numerical Methods for the Euler Equations of Fluid Dynamics*, (Eds. F. Angrand et. al.), SIAM, Philadelphia, 1985, pp. 199-245.

[12]Brandt, A. and Dinar, N., "Multigrid solution to elliptic flow problems," *Numerical Methodsa in PDE*, (Ed. S.V. Parter), Academic Press, New York, 1977, pp. 53-147.

[13]Fuchs, L., "Calculation of Flow Fields Using Overlapping Grids," *Notes on Numerical Fluid Mechanics*, (Ed. by P. Wesseling), Vol. 29, 1990, pp. 138-147.

[14]Chesshire, G. and Henshaw, W.D., "Composite Overlapping Meshes for the Solution of Partial Differential Equations," *J. Comput. Phys.*, Vol. 90, 1990, pp. 1-64.

[15]Sanatian, R., "The Experimental and Computational Simulation of Induction Flows in Spark Ignition Engines," *Ph.D. Thesis*, School of Mechanical Engineering, Cranfield Institute of Technology, UK. 1987.